Received: 28 January 2022 | Revised: 22 May 2023 | Accepted: 23 May 2023

DOI: 10.1002/hyp.14918

RESEARCH ARTICLE

WILEY

Rhine flood stories: Spatio-temporal analysis of historic and projected flood genesis in the Rhine River basin

Erwin Rottler[1,2] | Axel Bronstert[1] | Gerd Bürger[1] | Oldrich Rakovec[3,4]

[1]Institute of Environmental Science and Geography, University of Potsdam, Potsdam, Germany

[2]Department of Geography, University of Innsbruck, Innsbruck, Austria

[3]Department of Computational Hydrosystems, UFZ-Helmholtz Centre for Environmental Research, Leipzig, Germany

[4]Faculty of Environmental Sciences, Czech University of Life Sciences Prague, Prague, Czech Republic

Correspondence
Erwin Rottler, Department of Geography, University of Innsbruck, Innrain 52f, 6020 Innsbruck, Austria.
Email: erwin.rottler@uibk.ac.at

Abstract

The genesis of floods in large river basins often is complex. Streamflow originating from precipitation and snowmelt and different tributaries can superimpose and cause high water levels, threatening cities and communities along the riverbanks. For better understanding the mechanisms (origin and composition) of flood events in large and complex basins, we capture and share the story behind major historic and projected streamflow peaks in the Rhine River basin. Our analysis is based on hydrological simulations with the mesoscale Hydrological Model forced with both meteorological observations and an ensemble of climate projections. The spatio-temporal analysis of the flood events includes the assessment and mapping of antecedent liquid precipitation, snow cover changes, generated and routed runoff, areal extents of events, and the above-average runoff from major sub-basins up to 10 days before a streamflow peak. We introduce and assess the analytical setup by presenting the flood genesis of the two well-known Rhine floods that occurred in January 1995 and May 1999. We share our extensive collection of event-based Rhine River flood genesis, which can be used in- and outside the scientific community to explore the complexity and diversity of historic and projected flood genesis in the Rhine basin. An interactive web-based viewer provides easy access to all major historic and projected streamflow peaks at four locations along the Rhine. The comparison of peak flow genesis depending on different warming levels elucidates the role of changes in snow cover and precipitation characteristics in the (pre-)Alps for flood hazards along the entire channel of the Rhine. Furthermore, our results suggest a positive correlation between flood magnitudes and areal extents of an event. Further hydro-climatological research is required to improve the understanding of the climatic impact on the Rhine and beyond.

KEYWORDS

climate change, flood composition, flood genesis, mHM, model simulations, quantile extent, Rhine River, spatio-temporal analysis, web-based dashboard

1 | INTRODUCTION

Climatic changes are expected to alter flood hazard in river basins around the world (e.g., Bosshard et al., 2014; Bronstert, 2003; Di Sante et al., 2021; Didovets et al., 2019; Mtilatila et al., 2020; Muelchi et al., 2021; Thober et al., 2018; Vormoor et al., 2015). In order to reduce the risk for riparian communities from emerging hazards and to elucidate future developments of flood hazards, the understanding of the flood genesis is crucial (e.g., Berghuijs, Harrigan, et al., 2019; Brunner, Melsen, et al., 2020; Hundecha et al., 2020; Merz et al., 2021). A recent study by Blöschl (2022) discussing flood patterns across spatial scales further emphasizes the importance of research on this topic. Event-based investigations at the global scale, as conducted by Stein et al. (2020), provide a first structured glimps on flood composition and of climate change impacts on flood hazard at the continental scale. Analysis on the continental scale can partly refine the understanding of large scale flood genesis (e.g., Berghuijs et al., 2016; Berghuijs, Harrigan, et al., 2019; Brunner, Gilleland, et al., 2020; Huang et al., 2022; Jiang et al., 2022; Stein et al., 2021; Tarasova et al., 2023). Important hydrometeorological triggers for the generation of large-scale streamflow peaks include large-scale frontal rainstorms, convective rain cells over a large region, rainfall on a snow-covered landscape, and widespread snowmelt. In this context, we use the terminology "flood genesis "which comprises both the spatial origin of a flood event, as well as the mechanisms of origin. In the latter, we distinguish in particular the river runoff due to snowmelt and the runoff due to liquid precipitation that is, rain. Further detailing of flood-forming hydrological processes on and below the ground surface may be important, for example, for specific land surface runoff issues (Bronstert et al., 2023; Hundecha & Bárdossy, 2004; Niehoff et al., 2002), however, for the case of large river basins, where both pluvial and nival runoff generation may occur, the question of the extent, spatial origin, and timing of snowmelt and rain-induced runoff has prior importance for flood genesis. Therefore, in this study, we focus on the flood generation on the catchment scale and investigate the spatio-temporal distribution of rainfall, snowmelt and discharge generated.

In general, flood origin and composition in large river basins can be quite heterogeneous and difficult to capture. Large sets of observational data and/or model simulations are required to assess the flood genesis. Streamflow induced by precipitation and snowmelt and from different sub-basins can superimpose and cause high water levels (Fischer & Schumann, 2021; Guse et al., 2020; Kleinn et al., 2005; Ma et al., 2021); Disse and Engel (2001) demonstrate this for the Rhine basin. Furthermore, river training measures have the potential to affect flood magnitudes (Blöschl et al., 2015). Vorogushyn and Merz (2013) suggest that the construction of the Rhine weir cascade resulted in an acceleration of the Rhine flood waves, which might support unfavourable superpositions of peaks flows in the Rhine with flood waves from major tributaries. Increases in flood-producing precipitations can further increase flood hazards in the Rhine basin (Hurkmans et al., 2010; Pinter et al., 2006). Increases in rainfall sums also have the potential to increase the extent of an event. An increase in event extent can inter alia reflect an increase in contributing area (i.e., the area that provides runoff to the catchment outlet during an event) within a catchment (e.g., Fiorentino et al., 2007; Spence & Mengistu, 2019) or an increase in neighbouring river systems flooding at the same time (Berghuijs, Allen, et al., 2019; Kemter et al., 2020). In this study, we use the concept of contributing areas in the context of large-scale river flooding and assess the extent of an event within a catchment by identifying areas that played an important role during the flood genesis by generating large amounts of runoff.

In view of observed and projected changes in flood hazard, thorough flood risk estimates (e.g., te Linde et al., 2011) and strategies for a sustainable and transboundary flood management are required (Becker et al., 2007; Hooijer et al., 2004). A storyline approach can support the understanding and communication of potential risks (De Bruijn et al., 2016; Keller et al., 2018; Munz et al., 2022; Shepherd et al., 2018). However, until today, the analysis, visualization and presentation of flood genesis in complex basins remains challenging. Various variables need to be captured in space and time and presented concisely. In recent years, the potential of interactive web-based applications is more and more recognized and made use of in the scientific community (e.g., Dunning et al., 2017; Parding et al., 2020; Rottler, Vormoor, et al., 2021; Saha et al., 2021). An interactive web application also seems well suited to support the analysis and presentation of the flood genesis in large and complex river basins.

The main objective of this study is to conduct a comprehensive spatio-temporal analysis of historic and projected streamflow peak genesis in the Rhine basin. Therefore, we analyse model output from the mesoscale Hydrological Model (mHM; Kumar et al., 2013; Samaniego et al., 2010) forced with both historical meteorological forcing and an ensemble of climate projection scenarios. In order to capture the genesis of each major streamflow peak, we investigate simulated runoff at four gauges along the main channel of the Rhine, assess the above-average runoff from major sub-basins, estimate the importance of snowmelt and precipitation as flood formation mechanisms, assess the extent of each event, and map antecedent liquid precipitation, snow cover changes and generated and routed streamflow up to 10 days before a streamflow peak. We use the two well-known historic flood events occurring in January 1995 and May 1999 along the Rhine River to introduce the analytical tools and visualization techniques used in this study. The analysis goes along with developing an interactive web-based viewer that ensures easy access to the resulting figures and facilitates the comparison of streamflow peak genesis depending on location in the basin and forcing data. Furthermore, we group streamflow peaks according to warming levels and seasons to assess the systematic impacts of rising temperatures on the streamflow peak formation.

2 | STUDY AREA AND DATA

The Rhine basin is a large transboundary catchment in Central Europe (Figure 1 a). The river has great historic, economic and cultural value for the region and is an important waterway (Schiff, 2017; Uehlinger et al., 2009). Numerous large cities and industrial sites reside along the river. The basin encloses various different landscapes, including parts of

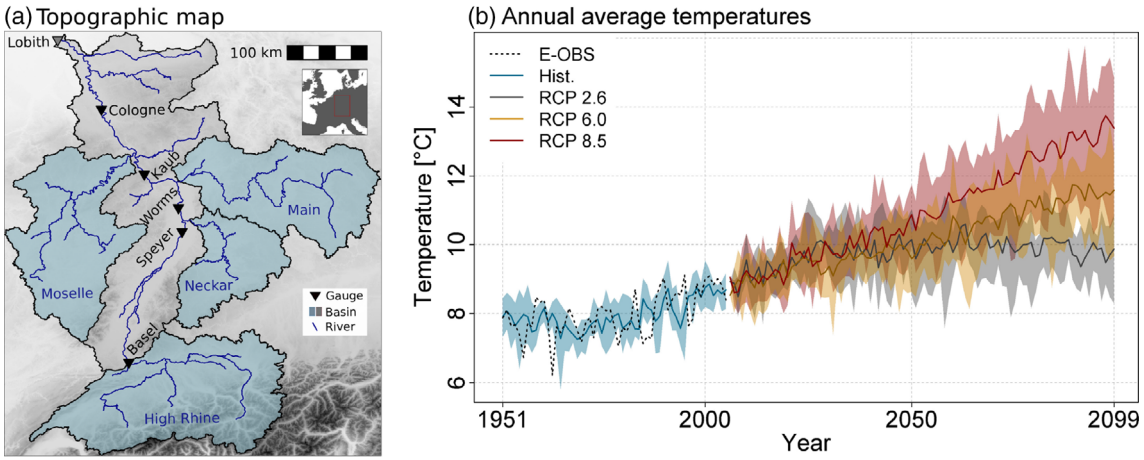

FIGURE 1 Topographic map of the Rhine River basin at Lobith with gauges and sub-basins investigated (a) and average annual temperatures in the Rhine River basin (b) for the historic (Hist.) time period (blue) and under three projected scenarios: RCP 2.6 (grey), 6.0 (orange) and 8.5 (red). Solid lines indicate the global climate model (GCM) ensemble mean, and the shaded area quantifies the range of the ensemble members. The black dotted line represents data based on observations (E-OBS).

the European Alps, German and French mid and low mountain ranges and lowland areas. Runoff originating from precipitation, snowmelt and ice-melt and from different tributaries superimpose in the main channel and create a complex flow regime (Stahl et al., 2016).

Our spatio-temporal analysis of historic and projected peak flow genesis in the basin is based on the hydrological modelling set-up presented in Rottler, Bronstert, et al. (2021). That study conducts hydrological simulations using the mesoscale hydrologic model (mHM) v.5.10 (Kumar et al., 2013; Samaniego et al., 2010). We use the extensive data pool from Rottler, Bronstert, et al. (2021) and perform a detailed analysis of individual, particularly high streamflow peaks and their genesis processes. So far, Rottler, Bronstert, et al. (2021) used the modelling set-up to assess projected changes in flood seasonality under global warming by calculating monthly and annual maxima and average annual cycles of selected variables and sub-basins. A detailed analysis of individual peaks, which is crucial to understand and pin down changes in flood genesis processes was still pending and is conducted here. No additional simulations with mHM are conducted in the framework of this study.

The multiscale parameter regionalisation (MPR) technique forms the core of the mHM model. In our model set-up, physiographic land surface predictors have a resolution of 500 m and the dominant hydrological processes are modelled at a 5 km spatial resolution. To ensure that rainfall- and snowmelt-driven runoff are represented well, Rottler, Bronstert, et al. (2021) calibrate the global parameters of the mHM model using a multi-basin calibration approach and validate at six additional river gauges using an independent evaluation period. The historical meteorological forcing is based on the E-OBS v12 gridded data sets (Haylock et al., 2008). Discharge observations used during model calibration and validation are obtained from the Global Runoff Data Centre (GRDC). Climate model data are taken from the Inter-Sectoral Impact Model Intercomparison Project (ISI-MIP) (Hempel et al., 2013; Warszawski et al., 2014) (Figure 1b). Note that climate models for the present do not reflect concrete observed events, but rather simulate realistic weather representative of a prescribed long-term climatology (e.g., 30-year averages). Within ISI-MIP, data from five global climate models (GCMs) are bias-corrected with a trend-preserving approach and interpolated to a 0.5° × 0.5° grid. The interpolation to a 5 km grid using external drift kriging was conducted within the project "End-to-end Demonstrator for improved decision making in the water sector in Europe" (EDgE) by order of the Copernicus Climate Service (Samaniego, Thober, et al., 2019). Detailed information on the multi-scale routing model (mRM) and the adaptive time step scheme (aTS) used for routing river runoff can be found in Thober et al. (2019).

3 | METHODS

3.1 | Rhine flood stories

The main objective of this study is to capture and share the flood genesis story behind major historic and projected streamflow peaks in the large and complex basin of the Rhine. Therefore, we assess the catchment dynamics in a sequence of analytical figures up to 10 days before the streamflow peak. The final figure of each sequence provides a quick yet comprehensive insight into the flood genesis. Analysing more than 4000 streamflow peaks from 101 catchments in Switzerland, Froidevaux et al. (2015) conclude that the consideration of 3–4 days prior to an event is sufficient to capture the flood-triggering precipitation in Swiss Alpine catchments. To account for larger catchment sizes, longer travel times and following investigations of Pinter et al. (2006), who suggest that 10-day antecedent precipitation best correlates with streamflow peaks at Cologne, we focus on catchment dynamics within a time window starting 10 days before a selected streamflow peak.

The spatio-temporal analysis includes the visualization of simulated streamflow at four locations along the Rhine River that is, Speyer, Worms, Kaub and Cologne, and of the four sub-basins of the High Rhine, Moselle, Neckar and Main River (Figure 1). This selection enables

the detection of source regions of routed streamflow and the tracking of streamflow superposition along the main channel of the Rhine River. In order to enable a direct comparison of the different locations and to avoid over/underestimations due to seasonal differences, we display streamflow as the fraction of the long-term median average for a given day simulated for the time frame 1951–2000 using E-OBS-based meteorological forcing. For example, streamflow simulated on the first of January is divided by the median average of the 50 values of streamflow simulated on the first of January between 1951 and 2000. For historic model simulations based on meteorological observations, we add observed discharge for locations that correspond to an existing river gauge that is, Cologne, Kaub, Worms, Speyer and Basel. The simulated streamflows for the tributaries Moselle, Neckar and Main are taken just before the confluence with the main channel of the Rhine River and do not reflect actual existing river gauges.

Furthermore, we calculate the cumulative above-average runoff from the sub-basins of the High Rhine, Neckar, Main and Moselle up to 10 days before the selected streamflow peak. We define above-average runoff as runoff above the long-term median average for a given day simulated for the time frame 1951–2000 using E-OBS-based meteorological forcing and estimate the importance of precipitation and snowmelt based on liquid precipitation and snowmelt in the respective sub-basin during peak flow formation. The long-term median average for the first of January, for example, is based on the 50 values simulated on the first of January between 1951 and 2000 using E-OBS-based meteorological forcing. The cumulative above-average runoff is calculated up to 10 days before the streamflow peak and depicted as a volume.

In addition, we calculate the fraction of upstream grid cells that at least once during the 10-day flood genesis period or the day of the peak itself generated runoff above a selected long-term quantile (quantile extent). We calculate this fraction for the 95%, 96%, 97%, 98% and 99% quantile. In the figure sequence, we display results for the 99% quantile. The long-term quantiles for grid cells were estimated using E-OBS-based simulations between 1951 and 2000. We assess quantile extents as an estimate of the spatial extent of an event. Maps of cumulative liquid precipitation, snow cover changes (snowmelt and snow accumulation) and generated and routed streamflow provide insights into the spatial patterns of the meteorological forcing data and streamflow generation. Cumulative values are calculated up to 10 days before the streamflow peak.

3.2 | Streamflow peak selection

We distinguish hydrological simulation runs based on the meteorological forcing data that is, observational data based on E-OBS, and climate model data from five GCMs for the historic time frame and three representative concentration pathways (RCPs) (Figure 2). This distinction results in 21 different forcing data. In the following, we determine the 10 highest streamflow peaks (mutually being at least 21 days apart to ensure the independence of the streamflow peaks) at four locations along the Rhine River (Speyer, Worms, Kaub and Cologne) in the 50-year time window 1951–2000 for the historical simulations and 2050–2099 for the climate projection scenarios. The selection of the 10 highest peaks ensures to keep the focus on the highest (potentially damaging) events, however, still enables the drawing of more general conclusion with regard to changes in the flood geneis, for example, due to rising temperatures. River gauges investigated are located before/after the confluence of one of the major tributaries (Figure 1). Hence, we investigate and prepare the sequence of analytical figures for 840 peaks (21 meteorological forcings × 4 locations × 10 streamflow peaks). As an example, in this article, we display the final figures of sequences depicting historic Rhine River floods recorded at Cologne in January 1995 (Figure 3) and Speyer in May 1999 (Figure 4). We select these two well-known rather severe flood events to make it easier for the reader to familiarize themselves with the presented analysis and visualization. The two flood events

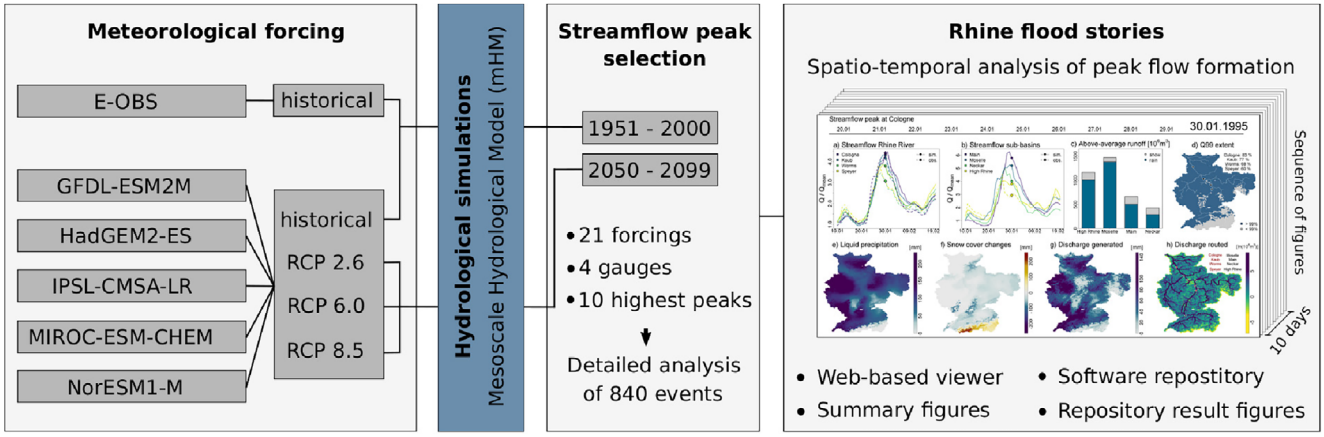

FIGURE 2 Schematic overview of the analytical set-up. We distinguish 21 different meteorological forcings that is, observational data based on E-OBS and climate model data from five global climate models (GCMs) for the historical time frame and three representative concentration pathways (RCPs). For four gauges along the Rhine River (Speyer, Worms, Kaub and Cologne), we selected 10 highest streamflow peaks for each forcing data.

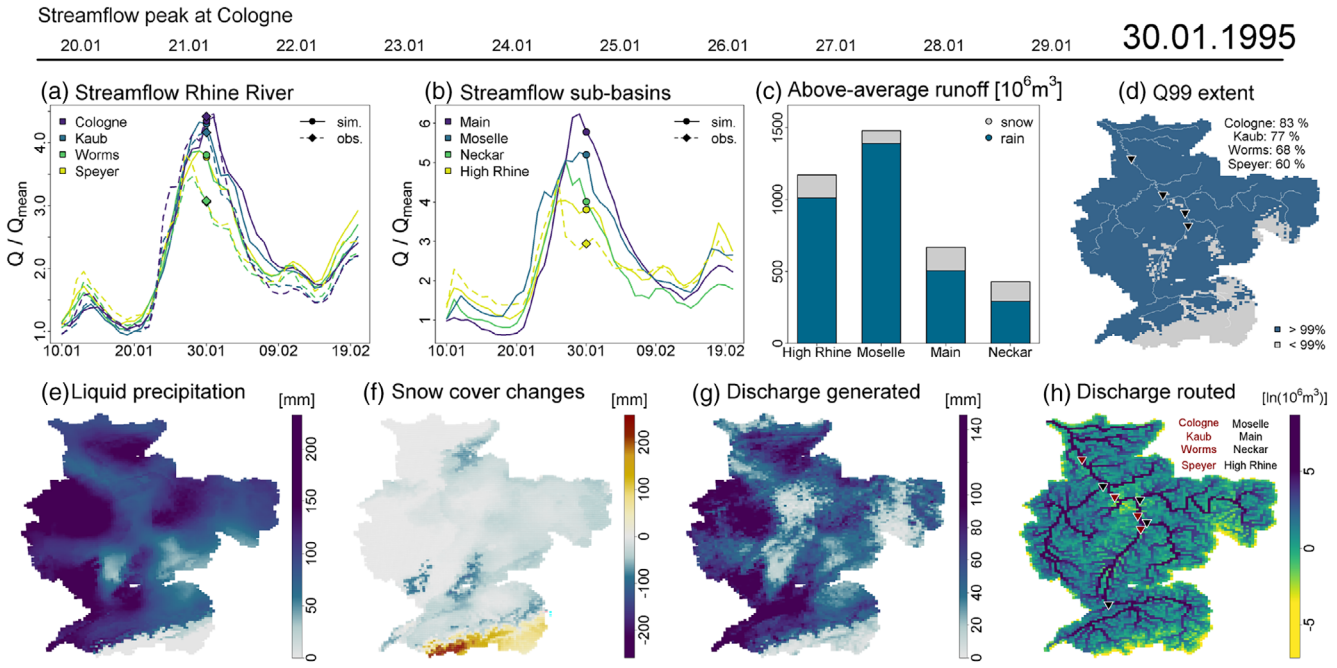

FIGURE 3 Spatio-temporal analysis of the streamflow peak in Cologne in January 1995 simulated using meteorological data sets based on observations (E-OBS) with (a) simulated and observed streamflow at Speyer, Worms, Kaub and Cologne, (b) simulated streamflow for the sub-basins High Rhine (observed values from gauge Basel), Neckar, Main and Moselle River (streamflows in a and b are displayed as the fraction of the long-term median average for a given day simulated for the time frame 1951–2000 using meteorological forcing based on E-OBS), (c) cumulative simulated above-average runoff up to 10 days before the streamflow peak that is, runoff above the long-term median average for a given day simulated for the time frame 1951–2000 using meteorological forcing based on E-OBS (rainfall and snowmelt contributions are estimated based on the amount of liquid precipitation and snowmelt in the sub-basins during peak formation), (d) Q99 extent estimated as the fraction of grid cells that generated runoff above their long-term 99% quantile (the long-term quantile has been estimated based on simulations for the time frame 1951–2000 using E-OBS-based meteorological forcing data), (e) cumulative liquid precipitation, (f) cumulative snow cover changes (snow accumulation and snowmelt), (g) cumulative discharge generated and (h) cumulative routed discharge (cumulative values in e–h are calculated up to 10 days before the streamflow peak).

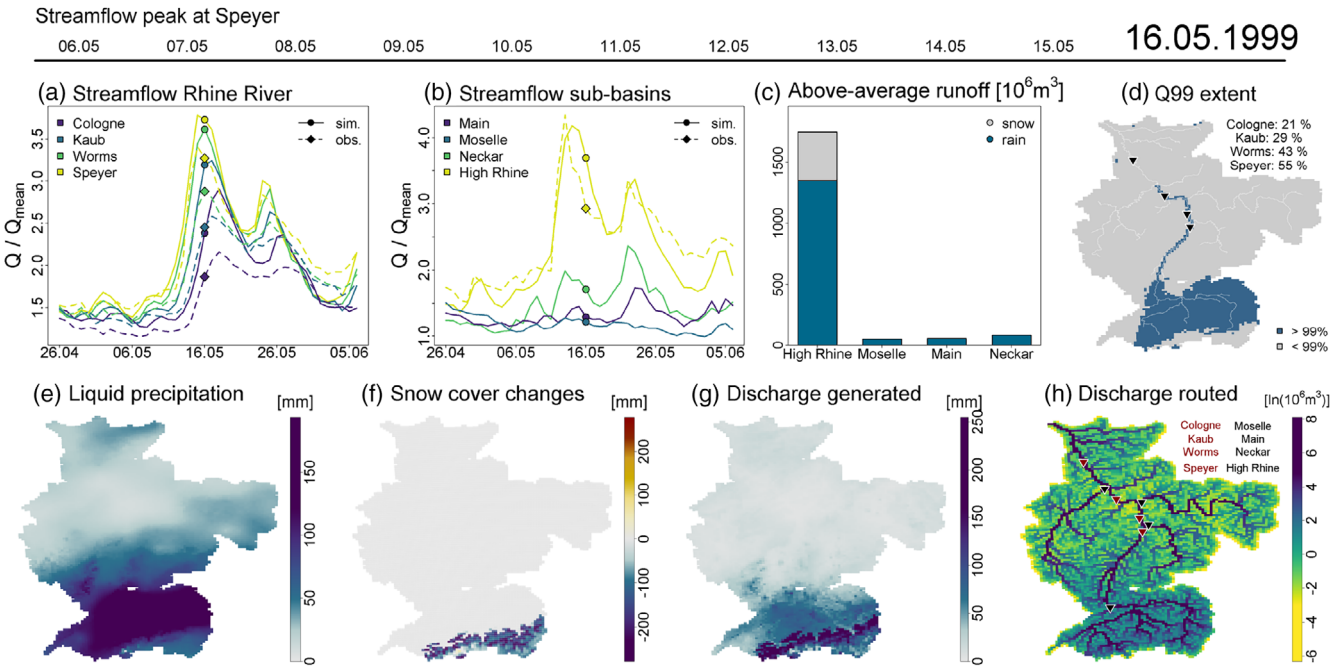

FIGURE 4 Same as Figure 3 but for the streamflow peak in Speyer in May 1999 simulated using gridded meteorological data sets based on observations (E-OBS).

are highest on record at the corresponding river gauges and an evaluation of results based on previous investigation is possible. In addition, we evaluate the simulations by calculating the Nash-Sutcliffe efficiency (NSE; Nash & Sutcliffe, 1970) and the Kling-Gupta-Efficiency (KGE; Gupta et al., 2009) for the streamflow peaks and their 10-day flood formation period.

3.3 | Interactive viewer

To ensure easy access to all results, we develop an interactive web-based dashboard based on the R package Shiny (Chang et al., 2019). The dashboard functions as a viewer displaying previously exported figure sequences. Furthermore, a short summary, figure descriptions, overview figures and contact details are available within the dashboard. An example of the web-viewer is available at http://natriskchange.ad.umwelt.uni-potsdam.de:3838/rhine-flood-genesis. All software code used to analyse and visualize the model output, including the interactive dashboard, is available at https://github.com/ERottler/rhine-flood-genesis. All figure sequences depicting the spatio-temporal analysis of historic and projected streamflow peaks investigated and a Docker image that enables the employment of the web application on local computers are available for download at https://doi.org/10.23728/b2share.d7595d0f30bd4335b0e5c1d9da474d37.

3.4 | Warming levels

In addition, we determine the warming level of each streamflow peak of a projected model run individually based on the average basin temperature within a centred 30-year moving window relative to temperatures based on observations between 1971 and 2000. For example, the warming level of a projected streamflow peak in the year 2060 is calculated by subtracting the observed basin mean average temperature between 1971 and 2000 from the projected average basin temperature between 2046 and 2075. As we do not have data beyond the year 2099, we allow for the calculations of averages within partial windows at the end of the time frame. Hence, the warming level of a streamflow peak simulated at the end of the total time frame, for example, the year 2095, is calculated by subtracting the basin mean average temperature between 1971 and 2000 from the average basin temperate between 2081 and 2099. Next, we group streamflow peaks following their individual warming level. We use the individual warming levels as a variable for grouping to assess the impact of rising temperatures on the streamflow peak formation.

For this type of analysis, we focus on streamflow peaks simulated at gauge Cologne, which is located at the Lower Rhine after the confluence of the Rhine River with all major tributaries investigated in this study. As a first step, we compare the average 10-day flood genesis process between October and March (Oct–Mar) and April to September (Apr–Sep). Aim of this seasonal comparison is to gain insights into the importance of snowmelt and precipitation from different areas of the basin depending of the time of occurrence. In the following, we will refer to events occurring between Oct and Mar (Apr–Sep) as cold-season (warm-season) floods. One-hundred and thirty streamflow peaks out of the 150 projected peaks at Cologne (5 GCMs × 3 RCPs × 10 highest peaks between 2050 and 2099) occurred between October and March. In a second step, we analyse the streamflow peaks occurring between October and March, which we consider to be more the winter-type floods, with regard to the flood genesis depending on rising temperatures. Main goal of this second comparison is to assess changes in the importance of snowmelt and precipitation as flood-contributing processes due to climate warming. In the selection period for projection scenarios (2050–2099), 58/72 peaks occur below/above a warming of 3°C. For selected groups of streamflow peaks, we calculate the average cumulative discharge generated, liquid precipitation and snow cover changes up to 10 days before the peaks for each raster cell in the basin and assess the difference between attained values. In the case of liquid precipitation, for example, we compute the average cumulative sum for the 58/72 events occurring below/above a warming of 3°C (and between October and March). Subsequently, we assess the difference of the group-specific averages. In order to assess (changes in) the importance of different sub-basin contributing to the streamflow peaks at gauge Cologne, we also compute cumulative above-average runoff, snowmelt and liquid precipitation up to 10 days before the event investigated in the High Rhine, Moselle, Neckar and Main for all streamflow peaks assessed for gauge Cologne. In this case, we again focus on the cold-season floods and differentiate between streamflow peaks below and above a warming of 3°C.

4 | RESULTS

4.1 | Spatio-temporal analysis

The January 1995 flood event of the Rhine went along with one of highest water levels ever recorded at gauge Cologne (Chbab, 1995; Fink et al., 1996) (Figure 3). The 10-day period prior to the streamflow peak is characterized by excessive rainfall, particularly in the Moselle catchment. In large parts of the Moselle catchment, three rainfall peaks accumulated to more than 150 mm of precipitation (Figure 3e). Snowmelt occurred in the mid and low mountain ranges (e.g., Vosges mountains and Black forest and parts of the Swiss Plateau), but it played only a minor role during flood genesis (Figure 3c,f). Over the Alpine ridge, precipitation was solid and accumulated in seasonal snow packs. 83% of the grid cells upstream gauge Cologne generated runoff above the long-term 99% quantile (Q99 extent) at least once during the 10-day flood genesis period or the day of the peak itself (Figure 3d). The direct comparison with observed values from river gauges along the Rhine suggests that the model was able to capture the rising limb of the flood event and the magnitudes at Kaub and Cologne well. The NSE/KGE value for the 10-day period prior to the event and the day of the event itself at gauge Cologne is 0.94/0.90. However, an overestimation of runoff in the falling limb, particularly in the High and Upper Rhine, showed up (Figure 3a,b).

The second presented example is the streamflow peak at gauge Speyer in May 1999 simulated using E-OBS-based data. The event in May 1999 represents the highest streamflow peak at gauge Speyer for the period 1951–2000. Strong snowmelt from the Alps superimposes heavy precipitation over pre-Alpine regions and the Swiss Plateau, causing very high runoff in the High and Upper Rhine. As intense precipitation and snowmelt were restricted to the High Rhine basin, the event did not play an important role downstream in the Middle and Lower Rhine. The direct comparison with observed values indicates that while the model was able to capture the rising limp of the event and the streamflow magnitudes in the High Rhine, streamflow peak magnitudes were increasingly overestimated going downstream the main channel of the Rhine. The NSE/KGE value for the 10-day period prior to the event and the day of the event itself at gauge Speyer is 0.89/0.78. The calculations of NSE and KGE between observed and modelled streamflow up to 10 days before the investigated streamflow of all peaks indicate that while the model seems to perform well in the Middle Rhine (Kaub) and Lower Rhine (Cologne), model performance decreases moving upstream the Upper Rhine (Worms and Speyer) (Figure 5).

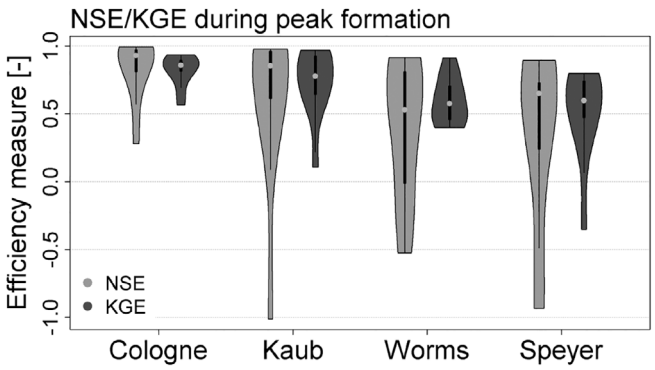

FIGURE 5 Nash-Sutcliffe efficiency (NSE) and Kling-Gupta efficiency (KGE) between observed and modelled runoff of the 10 historic events for river gauges Cologne, Kaub, Woms and Speyer. For each of the 10 historic events, the 10-day period before the streamflow peak and the day of the streamflow peak are considered for the analysis.

4.2 | Quantile extents

The comparison of quantile extents based on different probability levels indicates that during the 10-day streamflow peak genesis period, large parts of the upstream located watersheds are generating runoff above high long-term quantiles (Figure 6). In the case of Cologne, on average 86% of the grid cells generate runoff above the 95% quantile and on average 58% of the grid cells generate runoff above the 99% quantile (Figure 6a). In general, higher probability levels lead to higher quantile thresholds and lower quantile extents. At all four gauges investigated, large quantile extents positively correlate with streamflow peak magnitudes (Figure 7).

4.3 | Warming levels

During the formation of streamflow peaks recorded at Cologne between April and September (warm-season), snowmelt from the Alpine ridge seemed to play an important role in superimposing precipitation in the catchment (Figure 8a–c). Focusing on events occurring during the cold months between October and March, results indicate that the pre-Alpine and Alpine areas in the south of the basin

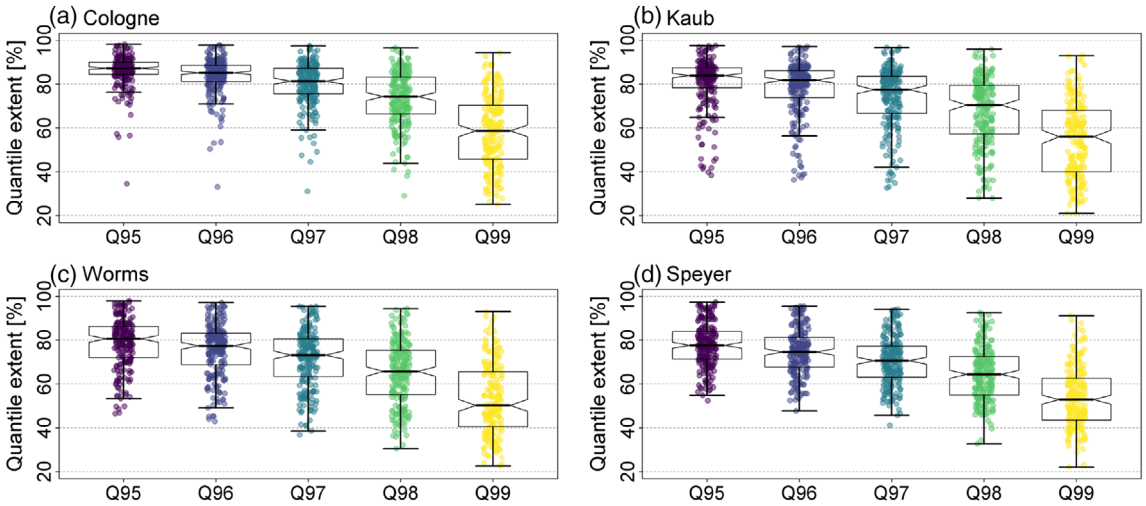

FIGURE 6 Fraction of grid cells upstream gauge Cologne (a), Kaub (b), Worms (c) and Speyer (d) generating runoff above the long-term 95%, 96%, 97%, 98%, and 99% quantile at least once in the 10 days before the selected streamflow peak or the day of the streamflow peak itself (quantile extent). Streamflow peaks of all 21 different meteorological forcings are considered. The long-term quantiles have been estimated based on simulations between 1951 and 2000 using E-OBS-based meteorological forcing.

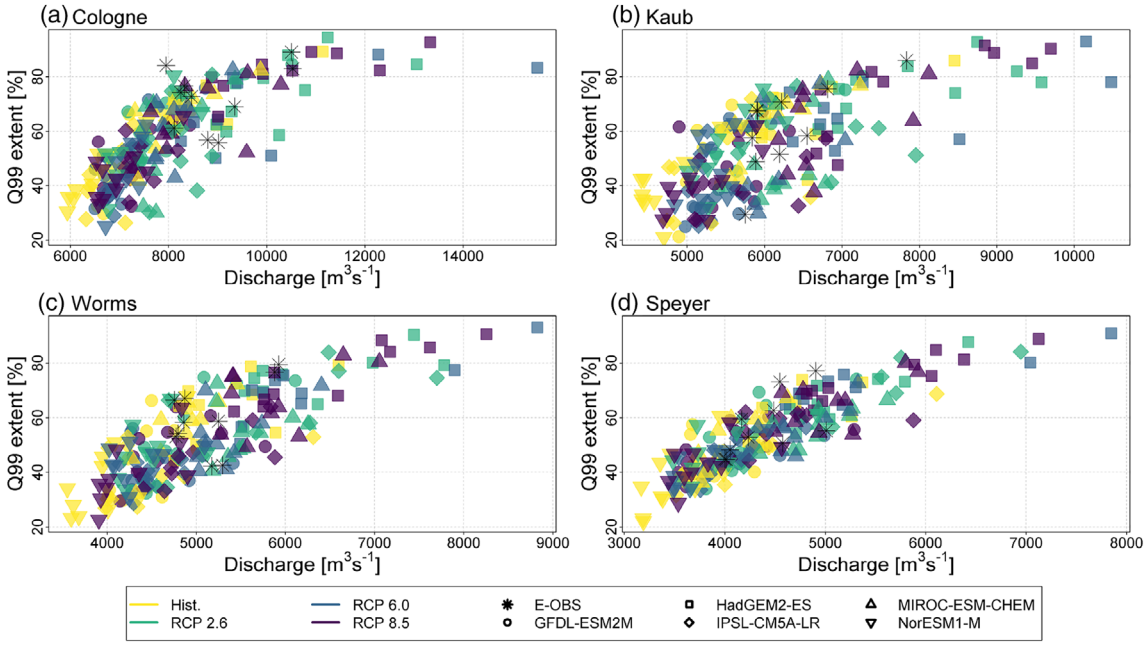

FIGURE 7 The magnitude and Q99 extent of the 10 highest streamflow peaks at Cologne (a), Kaub (b), Worms (c), and Speyer (d) simulated using different meteorological forcing data. The Q99 extent is estimated as the fraction of grid cells upstream of the selected location generating runoff above the long-term 99% quantile (long-term quantiles have been estimated based on simulations between 1951 and 2000 using E-OBS-based meteorological forcing). The streamflow peaks were selected between 1951 and 2000 for E-OBS-based and historical simulations and between 2050 and 2099 for model runs using representative concentration pathway (RCP) 2.6, 6.0, and 8.5. Point shapes represent different global climate model (GCM); colours indicate different RCPs.

react particularly strong to climate warming (Figure 8e). In these areas, increases in streamflow generation during peak formation seem to be caused by strong increases in liquid precipitation driven by an overall increase in precipitation sums reinforced by shifts from solid to liquid precipitation (reduced snow accumulation) (Figures 8g–i and 9) and snowmelt instead of accumulation (Figure 8j–l).

5 | DISCUSSION

5.1 | Rhine floods 1995 and 1999

The two well-known historic Rhine flood events of January 1995 and May 1999 presented in detail in this manuscript (Figures 3, 4) provide an insight into the analysis and visualization development of this study and give particular examples for the diversity of flood genesis processes along the Rhine. A detailed spatio-temporal analysis is crucial to pin down flow components and flood genesis areas driving the events. The sequence of analytical figures provides a quick yet comprehensive insight into the processes behind each streamflow peak. The flood in 1995 in Cologne was triggered by excessive rainfall over large areas of the basin, particularly in the sub-basin of the Moselle River. Over the Alps, precipitation was solid and accumulated as snow. This snow accumulation and storage prevented additional streamflow generation and even higher discharges. The investigation of the flood genesis in May 1999 points out that strong snowmelt from a high elevation, when superimposing with large rainfall sums, can cause very high streamflow peaks.

5.2 | Distinction between snowmelt and liquid precipitation

Our investigations suggest that the distinction between snowmelt and liquid precipitation and their mapping is an important condition for the understanding of the creation of a streamflow peak for the Rhine. Displaying simulated streamflows as the fraction of a long-term mean determined on a daily basis facilitates the comparison of locations in the basin and events. The quantification and visualization of above-average runoff and the estimation of contributions of snowmelt and liquid precipitation (e.g., Figure 3c) enable a quick assessment of the importance of different tributaries and runoff components.

5.3 | Potential for tracking streamflow components

In order to improve estimations of streamflow components, the next step could be the coupling of mHM to a streamflow component model (e.g., Stahl et al., 2016). By tracking the fraction of runoff components along the river network instead of estimating their

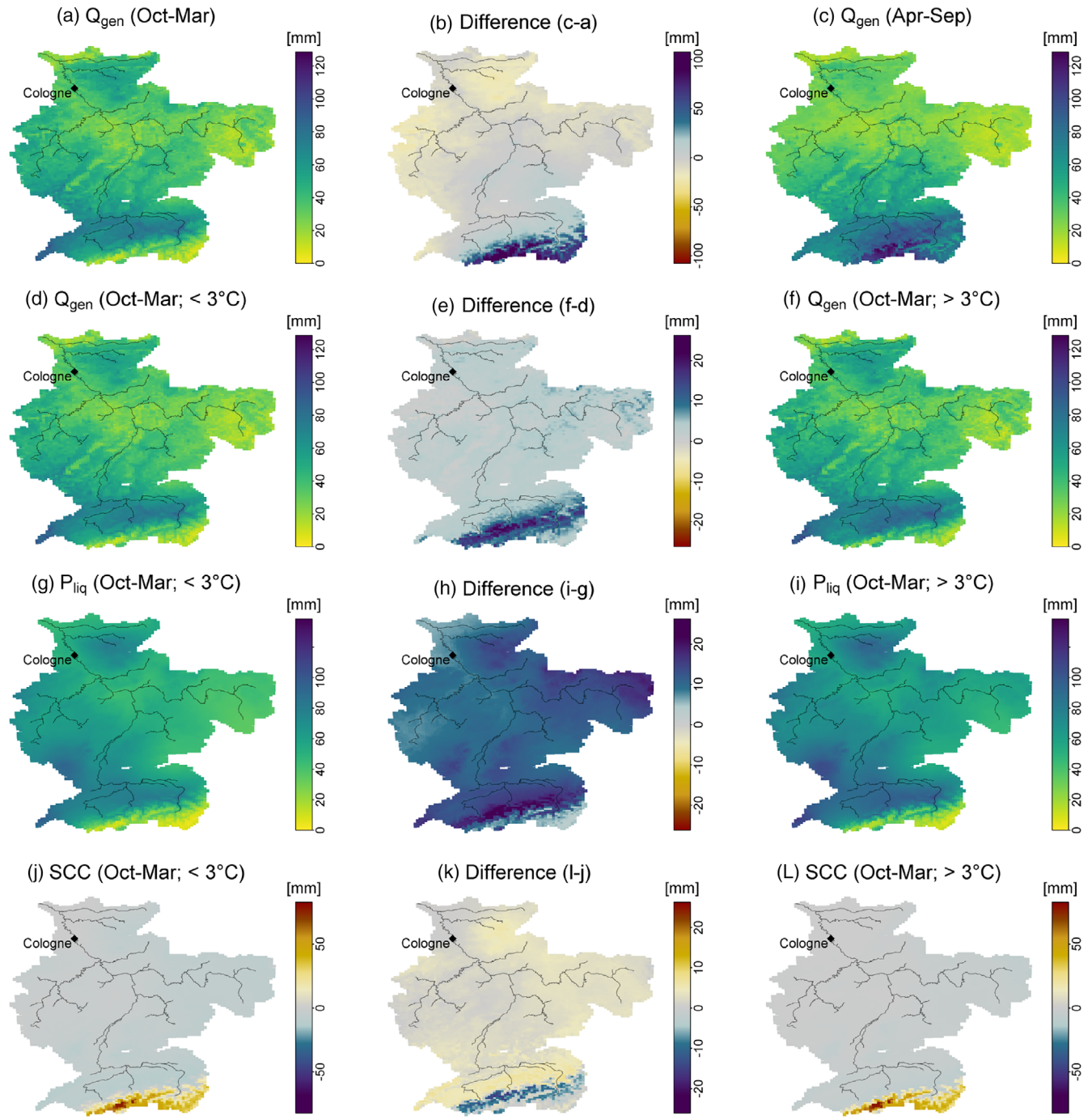

FIGURE 8 Maps of the average cumulative discharge generated (Qgen; a, c, d, and f), liquid precipitation (Pliq; g and i), and snow cover changes with positive/negative values indicating accumulation/melt (SSC; j and l) up to 10 days before the streamflow peak at Cologne. One-hundred and thirty peaks out of the 150 peaks (5 GCMs × 3 RCPs × 10 highest peaks between 2050 and 2099) occurred between October and March (Oct–Mar) and 20 peaks between April and September (Apr–Sep). Fifty-eight (72) simulated peaks between October and March occurred below (above) a 3°C warming (30-year average). The differences between seasons and warming levels, respectively, are depicted in (b, e, h, and k).

fraction based on gridded data of precipitation and snowmelt, the assessment of snowmelt and precipitation contributions to discharge at specific locations along the Rhine might be improved. Stahl et al. (2016), for example, successfully provided quantitative estimations of precipitation, snowmelt and glacier ice-melt components using 'virtual mixing tanks' throughout the model system.

5.4 | Comparison of quantile extents

The comparison of quantile extents based on different probability levels (i.e., 95%, 96%, 97%, 98%, and 99%) shows that the probability level selected needs to be sufficiently high to distinguish between different extreme events (Figure 6). Our results indicate that the 99%

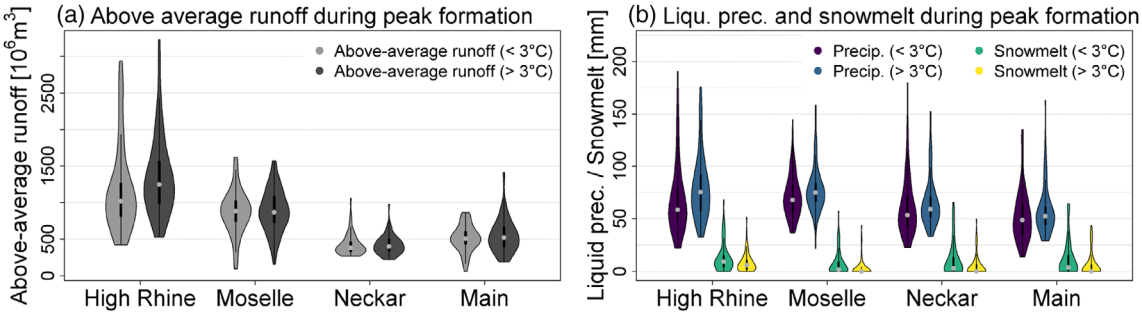

FIGURE 9 Cumulative above average runoff (a) and cumulative liquid precipitation and snowmelt (b) up to 10 days before the streamflow peaks simulated at gauge Cologne. 69 (81) of the 150 peaks considered (5 GCMs × 3 RCPs × 10 highest peaks between 2050 and 2099) occurred below (above) a 3°C warming (30-year average).

quantile seems an adequate threshold for quantile extent calculations. We want to point out that quantile extents do by no means provide information on inundated areas in the catchment. Fractions and maps solely indicate catchment areas that played an important role during the flood genesis by contributing large amounts of streamflow. The calculation of quantile extents requires a spatially distributed modelling approach. Our mapping and estimation of quantile extents point at increasing flood magnitudes with increasing quantile extent (Figure 7). Hence, high streamflow peaks only are possible when large parts of the basin contribute and generate very high levels of streamflow. We suggest that information on quantile extents from grid-based hydrological models can supplement analysis of the synchrony and spatial extent of flood events based on annual peak flows derived from streamflow recordings (e.g., Berghuijs, Allen, et al., 2019; Kemter et al., 2020).

5.5 | Changes in atmospheric circulation pattern

The positive correlation between flood magnitudes and quantile extents has to be kept in mind when assessing future changes in flood hazards for the Rhine. In addition to increasing liquid precipitation sums reinforced by shifts from solid to liquid precipitation (e.g., Pinter et al., 2006; Rottler, Bronstert, et al., 2021) (Figure 8), a warmer climate might lead to a weaker jet stream, which might allow circulation patterns to persist longer over Europe (Francis & Vavrus, 2015; Huguenin et al., 2020). Quasi-stationary conditions might favour high precipitation sums and increase the quantile extents and discharges. Investigating 122 mesoscale catchments in Germany, Petrow et al. (2009) point out that changes in frequency and persistence of circulation patterns directly influence the flood hazard. However, such changes in frequencies and persistence of atmospheric circulation types are not yet well represented in climate models (Huguenin et al., 2020). Further joint hydro-climatological research is required to improve our knowledge of the impact of changes in the persistence of circulation patterns on flood extent and hazard in the Rhine basin. The assessment of quantile extents based on distributed hydrological modelling can further support the quantification of such changes. By using generated streamflow by grid cell and not only the precipitation input, the interplay between precipitation, snowmelt and soil moisture, which has to be considered with regard to future changes in peak discharges and flood volumes (Brunner et al., 2019), can be accounted for.

5.6 | Relevance of precipitation and snowmelt characteristics in the (pre-)Alps

Furthermore, our analysis suggest that changes in precipitation characteristics and snowmelt in the (pre-)Alps are essential drivers of increases in streamflow peaks along the Rhine, also for cities like Cologne located at the Lower Rhine (Figure 8). In a warmer climate, higher temperatures move the snowline during flood formation upward, and larger areas in the High Rhine basin receive liquid instead of solid precipitation. This upward shift of the snowline leads to increased rainfall (liquid precipitation) sums (Figure 8h). A systematic investigation of the effect of rising temperatures on the freezing elevation in mountainous catchments, its impact on the fractions of liquid and solid precipitation, flood contributing areas and flood hazards can be found in Allamano et al. (2009). An overview summarizing the genesis of typical Rhine flood events (distinguishing cold and warm season) and potential changes due to rising temperatures as hypothesized within this study is given in Figure 10. We suggest that cold-season floods, which commonly are caused by large-scale advective precipitation events over large parts of the Rhine basin, might become more intense due to increasing precipitation sums and snowmelt instead of snow accumulation in the Alpine region. With regard to warm-season floods, we suggest that declining Alpine snowpacks might encounter more intense precipitation events (restricted to the southern part of the area). However, particularly with regard to warm-season flooding, further investigations are required to confirm these hypotheses. The analysis conducted within this study does not allow for a definite conclusion on this matter.

5.7 | Model limitations

The model performance evaluation using streamflow observations hints at limitations of the hydro-climatological model-set up to capture the full complexity of all major historic streamflow peaks. Particularly in the upstream areas, closer to the Alps, model performance becomes

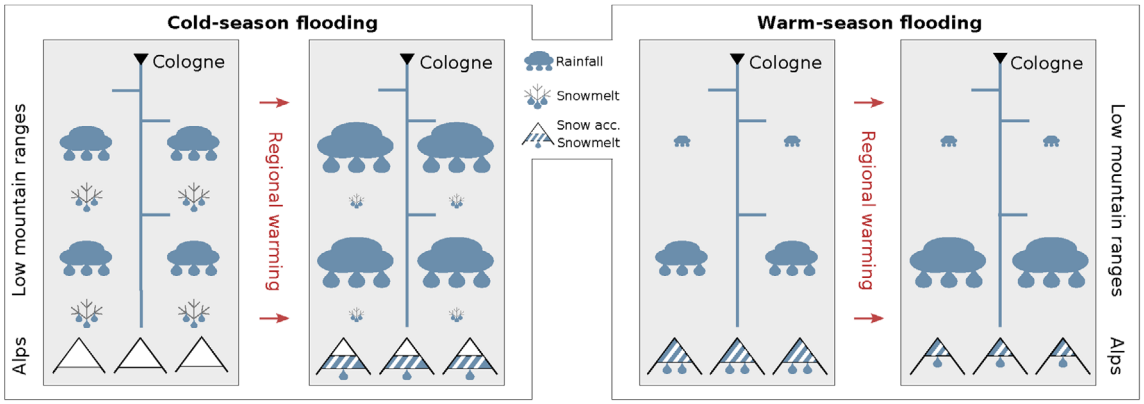

FIGURE 10 Schematic overview on the genesis of Rhine flood events, distinguishing cold and warm seasons, and potential changes of the flood genesis conditions due to regional climate warming.

weaker. In addition to the uncertainty in the gridded climatological input, particularly precipitation in high mountain areas, we suggest that this most likely is due to the lack of lake module and lake level regulation schemes in the model set-up. Furthermore, storage reservoirs for hydropower production are not yet implemented. The operation of storage reservoirs for hydropower generation has the potential to strongly impact streamflow seasonality along the Rhine (e.g., Rottler et al., 2020). Particularly for low flow analysis, the consideration of reservoir operations is indispensable (van Tiel et al., 2023). Another possible explanation for weaker model performance at the Upper Rhine gauges might be the relatively coarse model resolution of 5 km used to model high Alpine snow and hydrological processes. This coarse resolution can lead to large approximations in the complex terrain of the Alps, as mountain peaks, as well as valleys, are smoothed in the model set-up. Due to this limitation, the outcomes for the Alpine part rather have to be viewed as a synthetic hydrological modelling exercise investigating the potential impact of climatic changes than realistic representations of flood magnitudes. The weaker model performance in the Alpine part also limits the credibility of the model downstream the Rhine River. The good performance attested by evaluation metrics such as the NSE and KGE cannot guarantee that the physical processes are properly represented. However, we are confident to capture the large-scale dynamics with regard to precipitation, snowmelt and runoff generated well and that our analysis provides valuable new insights into (changes in) the processes generating peak flows in the Rhine River basin. For a reliable quantification of projected flood magnitudes, the usage of a model set-up including lake and reservoir modules is required. In addition to a quantification using the general extreme value distribution (Fisher & Tippett, 1928; Gumbel, 1958), the usage of metastatistical extreme value frameworks (Miniussi et al., 2020; Zorzetto et al., 2016) and physically-based extreme value distributions (Basso et al., 2021) should be considered.

5.8 | Access to all Rhine flood stories

The interactive viewer based on R Shiny ensured easy accessibility to all figure sequences produced. Software code is freely accessible and can be re-used and modified. All flood genesis stories, including a Docker image to run the web application locally, also can be downloaded from an open access data repository, which contains all analytical figures produced (https://doi.org/10.23728/b2share.d7595d0f30bd4335b0e5c1d9da474d37). To our knowledge, this represents the most comprehensive collection of event-based Rhine flood genesis information to date.

6 | CONCLUDING REMARKS AND OUTLOOK

6.1 | Spatio-temporal genesis of floods in a complex large river basin

Our analysis captures and presents the spatio-temporal evolution of 840 historic and projected streamflow peaks in the Rhine. The sequence of analytical figures exported for each streamflow peak enables a quick yet comprehensive insight into the peak genesis along the Rhine River. A detailed investigation and mapping of the spatio-temporal occurrence of precipitation and snow cover dynamics are crucial to understand the genesis of streamflow peaks along the Rhine through the different hydro-climatological regions. Our investigations point at the variety of possible precipitation and snowmelt sequences from different areas that can result in streamflow peaks in the large and complex basin of the Rhine River. A spatially distributed approach in an adequate resolution is necessary to enable a scientifically sound evaluation of hydrological extremes in this large basin and the future conditions to be expected. A possible pathway towards a comprehensive yet user-friendly visualization and assessment system has been presented here.

6.2 | Interactive visualization tool

The two well-known historic flood events occurring in January 1995 and May 1999 exemplary presented in detail in the manuscript provide insights into the analytical tools and visualization techniques developed and used in this study (Figures 3, 4). The interactive web-

based viewer and the online data repository ensure easy and long-term access to all result figures and a quick comparison of events forming at different locations along the Rhine and for different meteorological forcings. Our extensive collection of event-based Rhine flood genesis information can be used in- and outside the scientific community to explore and communicate the complexity and diversity of historic and projected flood genesis along the river.

6.3 | Importance of snowmelt and liquid precipitation

Furthermore, our results indicate that snow cover changes and changes in total precipitation and its liquid fraction in the (pre-)Alps are important drivers of changes in the flood hazard further downstream in the Middle and Lower Rhine (Figures 8–10). In a warmer climate, larger areas in the Alps seem to receive liquid instead of solid precipitation. This shift from solid to liquid precipitation increases precipitation totals and streamflow magnitudes along the Rhine.

6.4 | Future research perspectives

Our analysis also suggests a relationship between flood magnitudes and quantile extents. Further research is required to improve our knowledge about changes in the persistence of circulation patterns on flood extents and flood hazards for the Rhine. The calculation of quantile extents can support the quantification of changes in flood magnitudes due to changes in flood extents within future investigations. The model evaluation using observed streamflow points out the need to improve model performance in the Alpine part of the Rhine basin. The next steps need to incorporate lake retention effects and lake regulation schemes and the consideration of storage reservoirs for hydropower production. Furthermore, the hydrological model can be re-run with an updated and/or extended ensemble of climate projection scenarios and the mHM model coupled with a streamflow component model. The coupling with a streamflow component tracking approach has the potential to improve estimates of runoff components.

ACKNOWLEDGEMENTS

We acknowledge the data sets generated in the EDgE proof-of-concept project performed under a contract for the Copernicus Climate Change Service (https://climate.copernicus.eu/decision-making-water-sector-europe, last access: 03 November 2021). ECMWF implements this service and the Copernicus Atmosphere Monitoring Service on behalf of the European Commission. We acknowledge EDgE colleagues Luis Samaniego, Rohini Kumar and Stephan Thober for establishing the mHM model set-up and performing the downscaling of the CMIP5 data sets. We acknowledge the E-OBS data set from the EU FP6 project ENSEMBLES (http://ensembles-eu.metoffice.com, last access: 03 November 2021) and the data providers of the ECA&D project (http://www.ecad.eu, last access: 03 November 2021). We acknowledge the ISI-MIP project for providing the bias-corrected CMIP5 climate model data. The Copernicus Land Monitoring Service, implemented by the European Environmental Agency, provided the European Digital Elevation Model (EU-DEM), version 1.1. We also acknowledge the HOKLIM project (https://www.ufz.de/hoklim, last access: 03 November 2021) by the German Ministry for Education and Research (grant no. 01LS1611A). We thank the Global Runoff Data Centre (GRDC) for providing discharge observations. We also thank various other organizations and projects for providing data used in this study, including JRC, ESA, NASA, USGS, BGR, UNESCO, ISRIC and EEA. Open Access funding enabled and organized by Projekt DEAL.

CONFLICT OF INTEREST STATEMENT

The authors declare that they have no conflict of interest.

DATA AVAILABILITY STATEMENT

Source code of the hydrologic model mHM v.5.10 can be accessed at https://doi.org/10.5281/zenodo.3239055 (Samaniego, Kaluza, et al., 2019). R-scripts used to analyse simulation results including the web-based viewer are available at https://github.com/ERottler/rhine-flood-genesis. An example of the web-viewer is available at http://natriskchange.ad.umwelt.uni-potsdam.de:3838/rhine-flood-genesis. All figure sequences and a Docker image to run the web application locally are available for download at https://b2share.eudat.eu/records/72d7a4f5d38043d1a137228b39c7ecc3. Discharge data can be requested from the Global Runoff Data Centre (GRDC), 56 068 Koblenz, Germany. Further data sets used can be made available upon request.

ORCID

Erwin Rottler https://orcid.org/0000-0003-3072-2189
Axel Bronstert https://orcid.org/0000-0002-6369-8536
Gerd Bürger https://orcid.org/0000-0003-3539-2975
Oldrich Rakovec https://orcid.org/0000-0003-2451-3305

REFERENCES

Allamano, P., Claps, P., & Laio, F. (2009). Global warming increases flood risk in mountainous areas. *Geophysical Research Letters*, *36*, L24404.

Basso, S., Botter, G., Merz, R., & Miniussi, A. (2021). Phev! The physically-based extreme value distribution of river flows. *Environmental Research Letters*, *16*, 124065.

Becker, G., Aerts, J., & Huitema, D. (2007). Transboundary flood management in the Rhine basin: Challenges for improved cooperation. *Water Science and Technology*, *56*, 125–135.

Berghuijs, W. R., Allen, S. T., Harrigan, S., & Kirchner, J. W. (2019). Growing spatial scales of synchronous river flooding in Europe. *Geophysical Research Letters*, *46*, 1423–1428.

Berghuijs, W. R., Harrigan, S., Molnar, P., Slater, L. J., & Kirchner, J. W. (2019). The relative importance of different flood-generating mechanisms across Europe. *Water Resources Research*, *55*, 4582–4593.

Berghuijs, W. R., Woods, R. A., Hutton, C. J., & Sivapalan, M. (2016). Dominant flood generating mechanisms across the United States. *Geophysical Research Letters*, *43*, 4382–4390.

Blöschl, G. (2022). Flood generation: Process patterns from the raindrop to the ocean. *Hydrology and Earth System Sciences*, *26*, 2469–2480.

Blöschl, G., Gaál, L., Hall, J., Kiss, A., Komma, J., Nester, T., Parajka, J., Perdigão, R. A. P., Plavcová, L., Rogger, M., Salinas, J. L., & Viglione, A. (2015). Increasing river floods: Fiction or reality? *WIREs Water*, *2*, 329–344.

Bosshard, T., Kotlarski, S., Zappa, M., & Schär, C. (2014). Hydrological climate-impact projections for the Rhine River: GCM–RCM uncertainty and separate temperature and precipitation effects. *Journal of Hydrometeorology*, *15*, 697–713.

Bronstert, A. (2003). Floods and climate change: Interactions and impacts. *Risk Analysis*, *23*, 545–557.

Bronstert, A., Niehoff, D., & Schiffler, G. R. (2023). Modelling infiltration and infiltration excess: The importance of fast and local processes. *Hydrological Processes*, *37*, e14875.

Brunner, M. I., Gilleland, E., Wood, A., Swain, D. L., & Clark, M. (2020). Spatial dependence of floods shaped by spatiotemporal variations in meteorological and land-surface processes. *Geophysical Research Letters*, *47*, e2020GL088000.

Brunner, M. I., Hingray, B., Zappa, M., & Favre, A.-C. (2019). Future trends in the interdependence between flood peaks and volumes: Hydroclimatological drivers and uncertainty. *Water Resources Research*, *55*, 4745–4759.

Brunner, M. I., Melsen, L. A., Newman, A. J., Wood, A. W., & Clark, M. P. (2020). Future streamflow regime changes in the United States: Assessment using functional classification. *Hydrology and Earth System Sciences*, *24*, 3951–3966.

Chang, W., Cheng, J., Allaire, J., Xie, Y., & McPherson, J. (2019). shiny: Web Application Framework for R. R package version 1.3.2. https://CRAN.R-project.org/package=shiny

Chbab, E. (1995). How extreme were the 1995 flood waves on the rivers Rhine and Meuse? *Physics and Chemistry of the Earth*, *20*, 455–458.

De Bruijn, K., Lips, N., Gersonius, B., & Middelkoop, H. (2016). The storyline approach: A new way to analyse and improve flood event management. *Natural Hazards*, *81*, 99–121.

Di Sante, F., Coppola, E., & Giorgi, F. (2021). Projections of river floods in Europe using EURO-CORDEX, CMIP5 and CMIP6 simulations. *International Journal of Climatology*, *41*, 3203–3221.

Didovets, I., Krysanova, V., Bürger, G., Snizhko, S., Balabukh, V., & Bronstert, A. (2019). Climate change impact on regional floods in the Carpathian region. *Journal of Hydrology: Regional Studies*, *22*, 100590.

Disse, M., & Engel, H. (2001). Flood events in the Rhine basin: Genesis, influences and mitigation. *Natural Hazards*, *23*, 271–290.

Dunning, M. J., Vowler, S. L., Lalonde, E., Ross-Adams, H., Boutros, P., Mills, I. G., Lynch, A. G., & Lamb, A. D. (2017). Mining human prostate cancer datasets: The "camcAPP" shiny app. *eBioMedicine*, *17*, 5–6.

Fink, A., Ulbrich, U., & Engel, H. (1996). Aspects of the january 1995 flood in Germany. *Weather*, *51*, 34–39.

Fiorentino, M., Manfreda, S., & Iacobellis, V. (2007). Peak runoff contributing area as hydrological signature of the probability distribution of floods. *Advances in Water Resources*, *30*, 2123–2134.

Fischer, S., & Schumann, A. H. (2021). Multivariate flood frequency analysis in large river basins considering tributary impacts and flood types. *Water Resources Research*, *57*, e2020WR029029.

Fisher, R. A., & Tippett, L. H. C. (1928). Limiting forms of the frequency distribution of the largest or smallest member of a sample. *Mathematical Proceedings of the Cambridge Philosophical Society*, *24*, 180–190.

Francis, J. A., & Vavrus, S. J. (2015). Evidence for a wavier jet stream in response to rapid Arctic warming. *Environmental Research Letters*, *10*, 014005.

Froidevaux, P., Schwanbeck, J., Weingartner, R., Chevalier, C., & Martius, O. (2015). Flood triggering in Switzerland: The role of daily to monthly preceding precipitation. *Hydrology and Earth System Sciences*, *19*, 3903–3924.

Gumbel, E. J. (1958). *Statistics of extremes*. Columbia University Press.

Gupta, H. V., Kling, H., Yilmaz, K. K., & Martinez, G. F. (2009). Decomposition of the mean squared error and nse performance criteria: Implications for improving hydrological modelling. *Journal of Hydrology*, *377*, 80–91.

Guse, B., Merz, B., Wietzke, L., Ullrich, S., Viglione, A., & Vorogushyn, S. (2020). The role of flood wave superposition in the severity of large floods. *Hydrology and Earth System Sciences*, *24*, 1633–1648.

Haylock, M. R., Hofstra, N., Klein Tank, A. M. G., Klok, E. J., Jones, P. D., & New, M. (2008). A European daily high-resolution gridded data set of surface temperature and precipitation for 1950–2006. *Journal of Geophysical Research-Atmospheres*, *113*, D20119.

Hempel, S., Frieler, K., Warszawski, L., Schewe, J., & Piontek, F. (2013). A trend-preserving bias correction–The ISI-MIP approach. *Earth System Dynamics*, *4*, 219–236.

Hooijer, A., Klijn, F., Pedroli, G. B. M., & Van Os, A. G. (2004). Towards sustainable flood risk management in the Rhine and Meuse river basins: Synopsis of the findings of IRMA-SPONGE. *River Research and Applications*, *20*, 343–357.

Huang, H., Fischella, M. R., Liu, Y., Ban, Z., Fayne, J. V., Li, D., Cavanaugh, K. C., & Lettenmaier, D. P. (2022). Changes in mechanisms and characteristics of western U.S. floods over the last sixty years. *Geophysical Research Letters*, *49*, e2021GL097022.

Huguenin, M. F., Fischer, E. M., Kotlarski, S., Scherrer, S. C., Schwierz, C., & Knutti, R. (2020). Lack of change in the projected frequency and persistence of atmospheric circulation types over central europe. *Geophysical Research Letters*, *47*, e2019GL086132.

Hundecha, Y., & Bárdossy, A. (2004). Modeling of the effect of land use changes on the runoff generation of a river basin through parameter regionalization of a watershed model. *Journal of Hydrology*, *292*, 281–295.

Hundecha, Y., Parajka, J., & Viglione, A. (2020). Assessment of past flood changes across europe based on flood-generating processes. *Hydrological Sciences Journal*, *65*, 1830–1847.

Hurkmans, R., Terink, W., Uijlenhoet, R., Torfs, P., Jacob, D., & Troch, P. A. (2010). Changes in streamflow dynamics in the Rhine Basin under three high-resolution regional climate scenarios. *Journal of Climate*, *23*, 679–699.

Jiang, S., Bevacqua, E., & Zscheischler, J. (2022). River flooding mechanisms and their changes in europe revealed by explainable machine learning. *Hydrology and Earth System Sciences*, *26*, 6339–6359.

Keller, L., Rössler, O., Martius, O., & Weingartner, R. (2018). Delineation of flood generating processes and their hydrological response. *Hydrological Processes*, *32*, 228–240.

Kemter, M., Merz, B., Marwan, N., Vorogushyn, S., & Blöschl, G. (2020). Joint trends in flood magnitudes and spatial extents across Europe. *Geophysical Research Letters*, *47*, e2020GL087464.

Kleinn, J., Frei, C., Gurtz, J., Lüthi, D., Vidale, P. L., & Schär, C. (2005). Hydrologic simulations in the Rhine basin driven by a regional climate model. *Journal of Geophysical Research-Atmospheres*, *110*, D04102.

Kumar, R., Samaniego, L., & Attinger, S. (2013). Implications of distributed hydrologic model parameterization on water fluxes at multiple scales and locations. *Water Resources Research*, *49*, 360–379.

Ma, Q., Xiong, L., Xu, C.-Y., Li, R., Ji, C., & Zhang, Y. (2021). Flood wave superposition analysis using quantitative matching patterns of peak magnitude and timing in response to climate change. *Water Resources Management*, *35*, 2409–2432.

Merz, B., Blöschl, G., Vorogushyn, S., Dottori, F., Aerts, J. C., Bates, P., Bertola, M., Kemter, M., Kreibich, H., Lall, U., et al. (2021). Causes, impacts and patterns of disastrous river floods. *Nature Reviews Earth & Environment*, *2*, 592–609.

Miniussi, A., Marani, M., & Villarini, G. (2020). Metastatistical extreme value distribution applied to floods across the continental United States. *Advances in Water Resources*, *136*, 103498.

Mtilatila, L., Bronstert, A., Shrestha, P., Kadewere, P., & Vormoor, K. (2020). Susceptibility of water resources and hydropower production to climate change in the tropics: The case of Lake Malawi and Shire River basins, SE Africa. *Hydrology*, *7*, 54.

Muelchi, R., Rössler, O., Schwanbeck, J., Weingartner, R., & Martius, O. (2021). River runoff in Switzerland in a changing climate—Changes in moderate extremes and their seasonality. *Hydrology and Earth System Sciences*, *25*, 3577–3594.

Munz, L., Martius, O., Kauzlaric, M., Mosimann, M., Fehlmann, A., & Zischg, A. (2022). Participatory Development of Storymaps to Illustrate the Spatiotemporal Dynamics and Impacts of Extreme Flood Events, EGU General Assembly 2022, Vienna, Austria, 23–27 May 2022, EGU22-9712; 2022. https://doi.org/10.5194/egusphere-egu22-9712.

Nash, J. E., & Sutcliffe, J. V. (1970). River flow forecasting through conceptual models part I — A discussion of principles. *Journal of Hydrology*, *10*, 282–290.

Niehoff, D., Fritsch, U., & Bronstert, A. (2002). Land-use impacts on storm-runoff generation: Scenarios of land-use change and simulation of hydrological response in a meso-scale catchment in sw-Germany. *Journal of Hydrology*, *267*, 80–93.

Parding, K. M., Dobler, A., McSweeney, C. F., Landgren, O. A., Benestad, R., Erlandsen, H. B., Mezghani, A., Gregow, H., Räty, O., Viktor, E., El Zohbi, J., Christensen, O. B., & Loukos, H. (2020). GCMeval—An interactive tool for evaluation and selection of climate model ensembles. *Climate Services*, *18*, 100167.

Petrow, T., Zimmer, J., & Merz, B. (2009). Changes in the flood hazard in Germany through changing frequency and persistence of circulation patterns. *Natural Hazards and Earth System Sciences*, *9*, 1409–1423.

Pinter, N., van der Ploeg, R. R., Schweigert, P., & Hoefer, G. (2006). Flood magnification on the river Rhine. *Hydrological Processes*, *20*, 147–164. https://doi.org/10.1002/hyp.5908

Rottler, E., Bronstert, A., Bürger, G., & Rakovec, O. (2021). Projected changes in Rhine River flood seasonality under global warming. *Hydrology and Earth System Sciences*, *25*, 2353–2371.

Rottler, E., Francke, T., Bürger, G., & Bronstert, A. (2020). Long-term changes in central European river discharge for 1869–2016: Impact of changing snow covers, reservoir constructions and an intensified hydrological cycle. *Hydrology and Earth System Sciences*, *24*, 1721–1740.

Rottler, E., Vormoor, K., Francke, T., & Bronstert, A. (2021). Hydro explorer: An interactive web app to investigate changes in runoff timing and runoff seasonality all over the world. *River Research and Applications*, *37*, 544–554.

Saha, T. R., Shrestha, P. K., Rakovec, O., Thober, S., & Samaniego, L. (2021). A drought monitoring tool for South Asia. *Environmental Research Letters*, *16*, 54014.

Samaniego, L., Kaluza, M., Kumar, R., Rakovec, O., Schüler, L., Schweppe, R., Shrestha, P. K., Thober, S. and Attinger, S. (2019) *Mesoscale hydrologic model (v5.10)*. Zenodo. https://doi.org/10.5281/zenodo.3239055.

Samaniego, L., Kumar, R., & Attinger, S. (2010). Multiscale parameter regionalization of a grid-based hydrologic model at the mesoscale. *Water Resources Research*, *46*, W05523.

Samaniego, L., Thober, S., Wanders, N., Pan, M., Rakovec, O., Sheffield, J., Wood, E. F., Prudhomme, C., Rees, G., Houghton-Carr, H., Fry, M., Smith, K., Watts, G., Hisdal, H., Estrela, T., Buontempo, C., Marx, A., & Kumar, R. (2019). Hydrological forecasts and projections for improved decision-making in the water sector in Europe. *Bulletin of the American Meteorological Society*, *100*, 2451–2471.

Schiff, J. S. (2017). The evolution of Rhine river governance: Historical lessons for modern transboundary water management. *Water History*, *9*, 279–294.

Shepherd, T. G., Boyd, E., Calel, R. A., Chapman, S. C., Dessai, S., Dima-West, I. M., Fowler, H. J., James, R., Maraun, D., Martius, O., Senior, C. A., Sobel, A. H., Stainforth, D. A., Tett, S. F. B., Trenberth, K. E., van den Hurk, B. J. J. M., Watkins, N. W., Wilby, R. L., & Zenghelis, D. A. (2018). Storylines: An alternative approach to representing uncertainty in physical aspects of climate change. *Climatic Change*, *151*, 555–571.

Spence, C., & Mengistu, S. G. (2019). On the relationship between flood and contributing area. *Hydrological Processes*, *33*, 1980–1992.

Stahl, K., Weiler, M., Kohn, I., Freudiger, D., Seibert, J., Vis, M., Gerlinger, K., & Böhm, M. (2016). *The snow and glacier melt components of streamflow of the river Rhine and its tributaries considering the influence of climate change. Synthesis Report I-25*. International Commission for the Hydrology of the Rhine Basin.

Stein, L., Clark, M. P., Knoben, W. J. M., Pianosi, F., & Woods, R. A. (2021). How do climate and catchment attributes influence flood generating processes? A large-sample study for 671 catchments across the contiguous USA. *Water Resources Research*, *57*, e2020WR028300.

Stein, L., Pianosi, F., & Woods, R. (2020). Event-based classification for global study of river flood generating processes. *Hydrological Processes*, *34*, 1514–1529.

Tarasova, L., Lun, D., Merz, R., Blöschl, G., Basso, S., Bertola, M., Miniussi, A., Rakovec, O., Samaniego, L., Thober, S., & Kumar, R. (2023). Shifts in flood generation processes exacerbate regional flood anomalies in europe. *Communications Earth & Environment*, *4*, 49.

te Linde, A. H., Bubeck, P., Dekkers, J. E. C., de Moel, H., & Aerts, J. C. J. H. (2011). Future flood risk estimates along the river Rhine. *Natural Hazards and Earth System Sciences*, *11*, 459–473.

Thober, S., Cuntz, M., Kelbling, M., Kumar, R., Mai, J., & Samaniego, L. (2019). The multiscale routing model mRM v1.0: Simple river routing at resolutions from 1 to 50 km. *Geoscientific Model Development*, *12*, 2501–2521.

Thober, S., Kumar, R., Wanders, N., Marx, A., Pan, M., Rakovec, O., Samaniego, L., Sheffield, J., Wood, E. F., & Zink, M. (2018). Multi-model ensemble projections of European river floods and high flows at 1.5, 2, and 3 degrees global warming. *Environmental Research Letters*, *13*, 014003.

Uehlinger, U. F., Wantzen, K. M., Leuven, R. S., & Arndt, H. (2009). The Rhine River basin. In K. Tockner (Ed.), *Rivers of Europe* (pp. 199–245). Academic Press.

van Tiel, M., Weiler, M., Freudiger, D., Moretti, G., Kohn, I., Gerlinger, K., & Stahl, K. (2023). Melting alpine water towers aggravate downstream low flows: A stress-test storyline approach. *Earth's Future*, *11*, e2022EF003408.

Vormoor, K., Lawrence, D., Heistermann, M., & Bronstert, A. (2015). Climate change impacts on the seasonality and generation processes of floods & projections and uncertainties for catchments with mixed snowmelt/rainfall regimes. *Hydrology and Earth System Sciences*, *19*, 913–931.

Vorogushyn, S., & Merz, B. (2013). Flood trends along the Rhine: The role of river training. *Hydrology and Earth System Sciences*, *17*, 3871–3884.

Warszawski, L., Frieler, K., Huber, V., Piontek, F., Serdeczny, O., & Schewe, J. (2014). The inter-sectoral impact model intercomparison project (ISI–MIP): Project framework. *Proceedings of the National Academy of Sciences*, *111*, 3228–3232.

Zorzetto, E., Botter, G., & Marani, M. (2016). On the emergence of rainfall extremes from ordinary events. *Geophysical Research Letters*, *43*, 8076–8082.

How to cite this article: Rottler, E., Bronstert, A., Bürger, G., & Rakovec, O. (2023). Rhine flood stories: Spatio-temporal analysis of historic and projected flood genesis in the Rhine River basin. *Hydrological Processes*, *37*(6), e14918. https://doi.org/10.1002/hyp.14918